Table 2. Before the test was carried out, the samples were measured using a Vernier caliper, and the compression plate was coated with Vaseline jelly as the lubricant to reduce the friction effect. Data collected from compression tests such as the load-displacement curves and the stress-strain curves were evaluated from each sample to analyze its mechanical properties, i.e. Young's modulus and ultimate strength.

Table 2. Samples dimension

Bioplastic with specific amount turmeric, % (w/w)	Dimension, cm
0.50	2×2×0.6
0.75	2×2×0.6
1.00	1.5×1.5×0.5
1.50	1.5×1.5×0.5

The following formula can be used to process the raw data from the compression test for further analyses:

(1) *Ultimate compressive strength* (S_{ucs}) is defined as the maximum force that can be held in the sample when being compressed before the material is broken. The ultimate compression strength can be calculated by dividing maximum stress (F_M; N) with the cross-section area of the specimen (A; mm^2)) as shown in Eq. (1) [34].

$$S_{ucs} = \frac{F_M}{A}. \tag{1}$$

(2) *Young's modulus* (E) is a mechanical property that measures the stiffness of elastic deformation of the specimen under a given load. Young's modulus can be obtained from the slope of the stress-strain since defines the relationship between stress (σ) and strain (ε) of material deformation in the linear elasticity regime. Young's modulus can be determined using Eq. (2) [34].

$$E = \frac{\sigma_2-\sigma_1}{\varepsilon_2-\varepsilon_1}, \tag{2}$$

where ε_1 and ε_2 are the condition of relative elongation, and σ_1 and σ_2 are the stress that occurs at ε_1 and ε_2, respectively. The method of observing the slope-strain of the sample for defining Young's modulus is adopted since the slope of the sample can be directly observed as a function of the material deformation (strain).

Biodegradability. The biodegradability tests were conducted by slicing the prepared bioplastics with sizes of about 5×5×5 mm and then immersing them into ultrapure water. The weight losses of the sample were measure at the interval time of two days. In line with this test, during the immersing process, it was also visually observed the change of color. Detailed information about the biodegradability test is reported in our previous study [35].

3. Results and Discussion

Figure 1 is a photograph of a bioplastic fabrication with the addition of the amount of turmeric. The addition of turmeric gives the bioplastic end product its yellow color. The amount of turmeric added affects the physical condition of the bioplastic, where the bioplastic with a higher amount of turmeric causes the bioplastic to crack (see Figs. 1 (a) 0.50; (b) 0.75; (c) 1.00; and (d) 1.50% (w/w)).

To clarify the bioplastic structure, a microscope analysis was conducted (See Fig. 2). The results in Figs. 2(a) and (b) are the appearances of the micron-sized cornstarch and turmeric powder that has been prepared. Micron-sized cornstarch is a white crystal, solid and dense. Turmeric powder is a yellow color, heterogeneous surface, and agglomerate. Figure 2(c), (d), (e), and (f) are bioplastics with addition of specific amount of turmeric of 0.50; 0.75; 1.00; and 1.50% (w/w), respectively. Bioplastics with the addition of a higher amount of turmeric have a more heterogeneous surface and agglomerates, making them more brittle and stiffer. Figure 2(g) is the appearance of the bioplastic after being immersed for two weeks in water. The color of the bioplastic starts to change from yellow to brownish-yellow. It can be seen that after two weeks of immersion, cracks are found due to the swelling phenomenon. Figure 2(h) is the appearance of the bioplastic after being immersed for four weeks in the water in which fungi grow significantly.

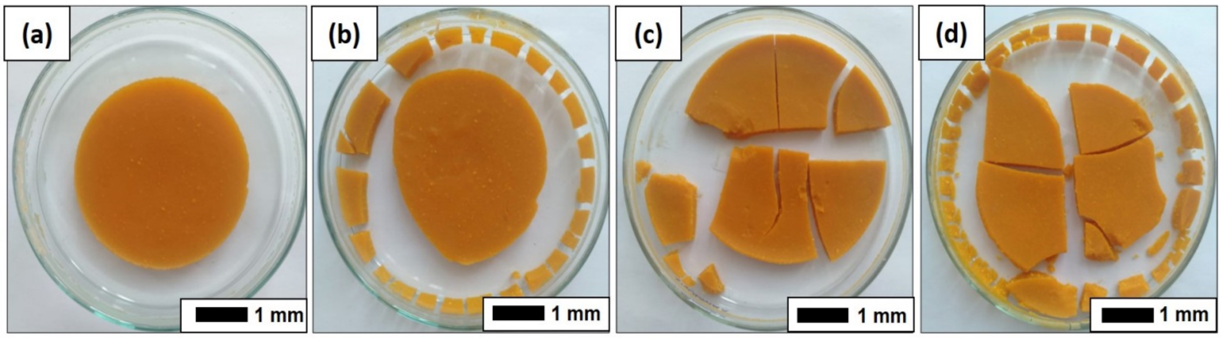

Fig. 1. Photograph image of cornstarch-based bioplastics with the addition specific amount turmeric (a) 0.50; (b) 0.75; (c) 1.00; and (d) 1.50% (w/w)

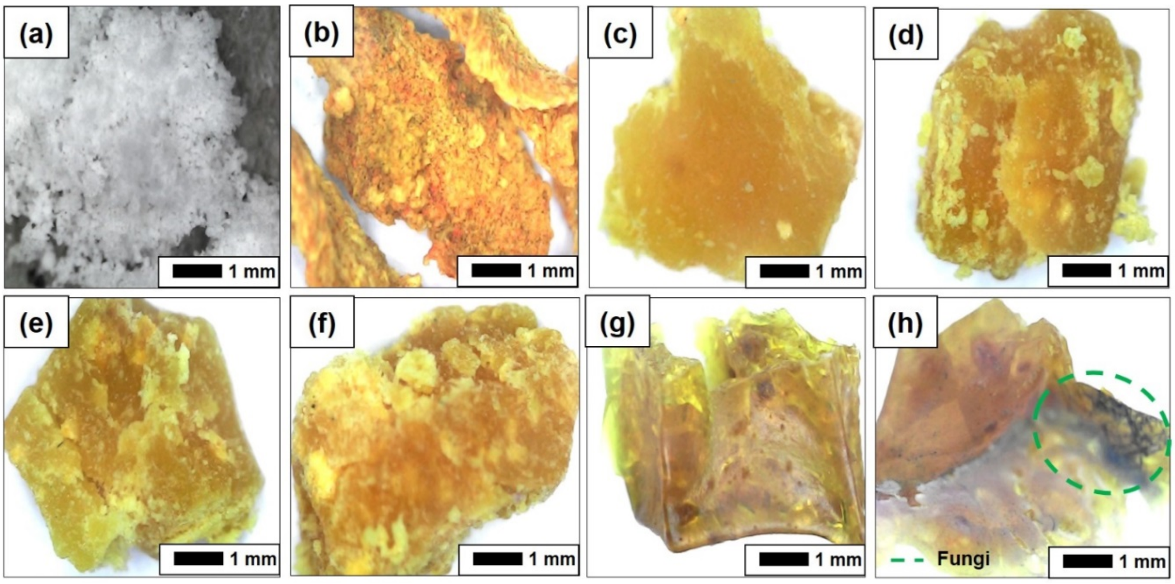

Fig. 2. Microscope image of sample: (a) micro-sized cornstarch, (b) agglomerated turmeric powder, (c-f) bioplastic with specific amount turmeric ((c) 0.50; (d) 0.75; (e) 1.00; and (e) 1.50% (w/w)), (g) bioplastics after two weeks immerged in water and (h) fungi bioplastic after four weeks immerged in water

To confirm the phenomenon during the immersion process, Fig. 3 shows the results of the FTIR analysis of as-prepared bioplastics, bioplastics immersed for two weeks in water, and the surface of the bioplastic samples immersed for four weeks. Data were then compared with the standard FTIR analysis [36]. The as-prepared bioplastic results were identified at wavelengths 1022, 1647, and 3280 cm^{-1}. A comparison of FTIR peaks for bioplastics before and after two weeks of immersion in water confirms that biodegradability in water is simply a dilution of the outer components of the bioplastic. The reaction between water and bioplastics involves a dilution process and does not interfere with complicated reactions. We also found that in the FTIR spectra of bioplastics after four weeks of immersion, the absorption peak experienced a decrease in intensity, indicating degradation that changed the chemical structure of bioplastics due to fungal activity.

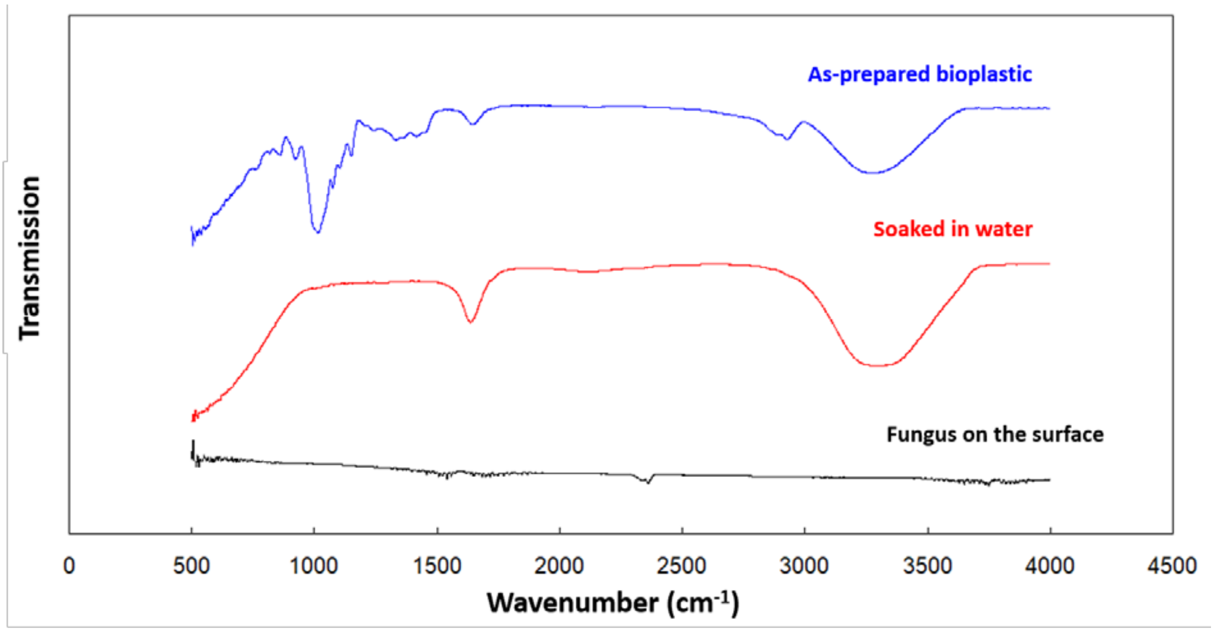

Fig. 3. FTIR analysis results of as-prepared bioplastic, 2-week immerged bioplastic in water, and fungus on the 4-week immerged sample

A biodegradability test of bioplastic samples with different turmeric amounts was carried out by immersion method [35]. It was evaluated by analyzing the mass of the bioplastics as a function of days. Table 3 shows the results of the bioplastic reduction performed for two weeks. The analysis showed that the sample with 0.50% (w/w) of turmeric had the best biodegradability, which was indicated by a weight loss of 86% for two weeks. The possible weight loss during 2-week immersion is because the bioplastics' outer surfaces were diluted in water, which was confirmed by the identical FTIR patterns. This result is different for 2-week immersion bioplastic, in which the mass loss was followed by the appearance of fungus (see Fig. 2(h)) and fungus chemical structure (see Fig. 3). The present bioplastics were made from cornstarch, making microorganisms to break the polymer chain easily inside the bioplastics themselves [37]. However, we found that the biodegradability of the present bioplastic is slower than that of bioplastic made from starch without additional curcumin [36]. The main reason is that the curcumin creates an antimicrobial agent, slowing the growth of microbes in degrading the bioplastic.

Figure 4 is a two-dimensional illustration model of particle crack during mechanical testing. The blue square and yellow circle represent the cornstarch and turmeric particle, respectively. The amount of turmeric added to the bioplastic fabrication process directly affects the mechanical and physical properties of the bioplastic. Due to the nature of a crack, the initiated crack propagates toward the turmeric particles because of the relatively low stiffness than cornstarch (see Fig. 4(a)) [38]. Furthermore, the bonding between cornstarch and turmeric is relatively low and easy to break [39]. This means the addition of turmeric amount could fasten the crack propagation (see Fig. 4(b)). However, when the turmeric particles are quite a lot, a polymerization between turmeric particles might occur, resulting in a higher stiffness of polymerized turmeric particles (see Fig. (4c)). As a consequence, the initiated crack tends to avoid the polymerized turmeric particles. To confirm these phenomena, compressive test for different turmeric amount was conducted.

Table 3. Weight loss bioplastics with the addition of a specific amount of turmeric during the immersion process

0.50% (w/w)	Days	Initial Dimension, cm^2	Initial mass, g	Mass after Immersion, g	Mass loss, wt%	Decay dimension, g/cm^2
	1	1.316	0.150	0.113	24	0.030
	2	1.311	0.093	0.043	55	0.039
	4	1.120	0.107	0.037	66	0.063
	6	1.254	0.133	0.040	71	0.075
	8	1.181	0.153	0.040	74	0.096
	10	1.283	0.143	0.027	81	0.092
	14	1.460	0.143	0.020	86	0.088
0.75% (w/w)	Days	Initial Dimension, cm^2	Initial mass, g	Mass after Immersion, g	Mass loss, wt%	Decay dimension, g/cm^2
	1	1.089	0.130	0.087	33	0.040
	2	1.364	0.127	0.077	40	0.039
	4	1.203	0.140	0.067	53	0.070
	6	1.071	0.147	0.057	61	0.085
	8	1.214	0.133	0.050	63	0.069
	10	0.939	0.107	0.037	66	0.075
	14	1.145	0.0133	0.037	73	0.086
1.00% (w/w)	Days	Initial Dimension, cm^2	Initial mass, g	Mass after Immersion, g	Mass loss, wt%	Decay dimension, g/cm^2
	1	1.106	0.147	0.090	39	0.052
	2	1.146	0.143	0.080	44	0.055
	4	0.887	0.127	0.063	50	0.071
	6	1.070	0.133	0.053	60	0.076
	8	1.038	0.140	0.053	62	0.085
	10	1.103	0.153	0.053	65	0.095
	14	1.101	0.143	0.043	70	0.093
1.50% (w/w)	Days	Initial Dimension, cm^2	Initial mass, g	Mass after Immersion, g	Mass loss, wt%	Decay dimension, g/cm^2
	1	1.378	0.137	0.103	24	0.025
	2	1.006	0.120	0.063	48	0.065
	4	1.192	0.110	0.047	57	0.057
	6	1.168	0.127	0.047	63	0.072
	8	1.276	0.123	0.043	65	0.063
	10	1.433	0.130	0.043	67	0.061
	14	1.249	0.130	0.040	69	0.075

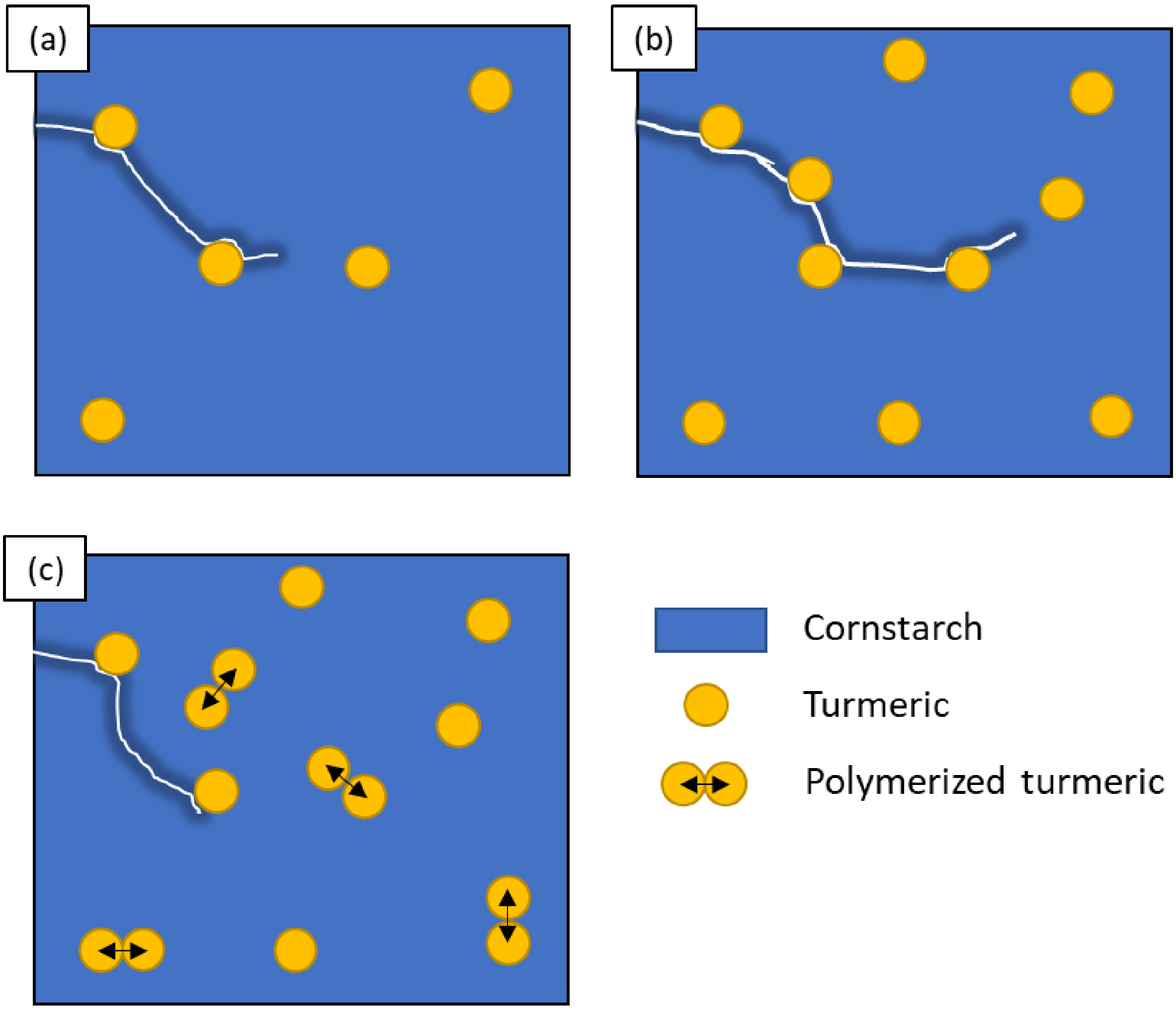

Fig. 4. Illustration progression cracking of bioplastic for (a) low density of turmeric, (b) high density of turmeric, and (c) high density of turmeric with polymerization

Figure 5 shows the plot of stress-strain data of the bioplastic sample from the compression test. Refer to Fig. 4, it can be observed that the stress-strain curve of each sample shows a similar trend by showing the elastic deformation region and followed by the ultimate stress (peak stress). The observation will be focused on the ultimate strength as it represents the maximum compression force per unit cross-section area that the sample can survive before breaking up.

To observe the ultimate strength of each sample, the stress-strain plot was particularly limited to the strain of 0.6 and stress of 2250 kPa, as presented in Fig. 6. The ultimate strength values can be then determined as shown in Table 4. The ultimate strength values of samples of 0.50; 0.75; and 1.00% (w/w) were 1059.0; 941.2; and 375.8 kPa, respectively, showing a decreasing trend of strength with increasing turmeric addition. It decreased because the turmeric particle has low stiffness and low bonding strength with cornstarch. As a result, it fastens the crack propagation and resulting in lower compressive strength. However, sample 1.50% (w/w) shows a different behavior of having the ultimate strength of 1957.0 kPa. It might be due to the high turmeric content in the material, which increased the potency of turmeric particles to do the polymerization process (see Fig. 4(c)), causing a higher stiffness. The high stiffness can resist crack propagation inside the bioplastics. This behavior was then confirmed by observing Young's moduli values of each bioplastic sample under compressive load.

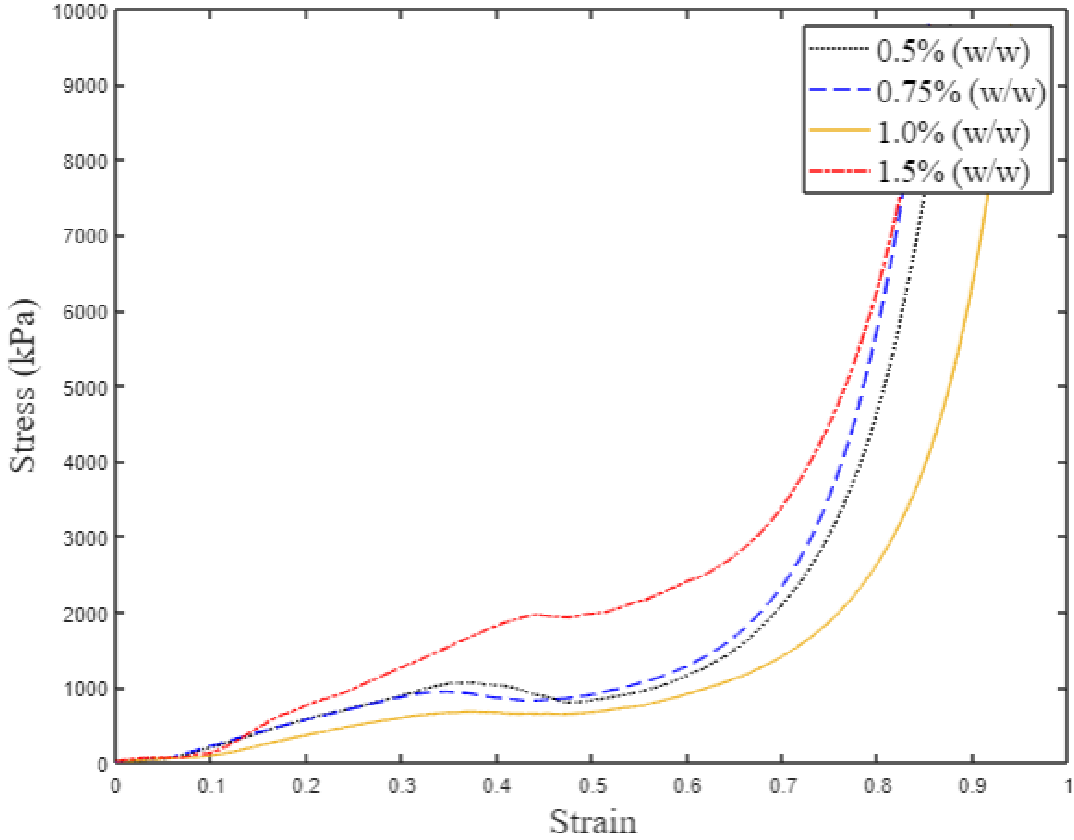

Fig. 5. Stress vs strain of bioplastic samples

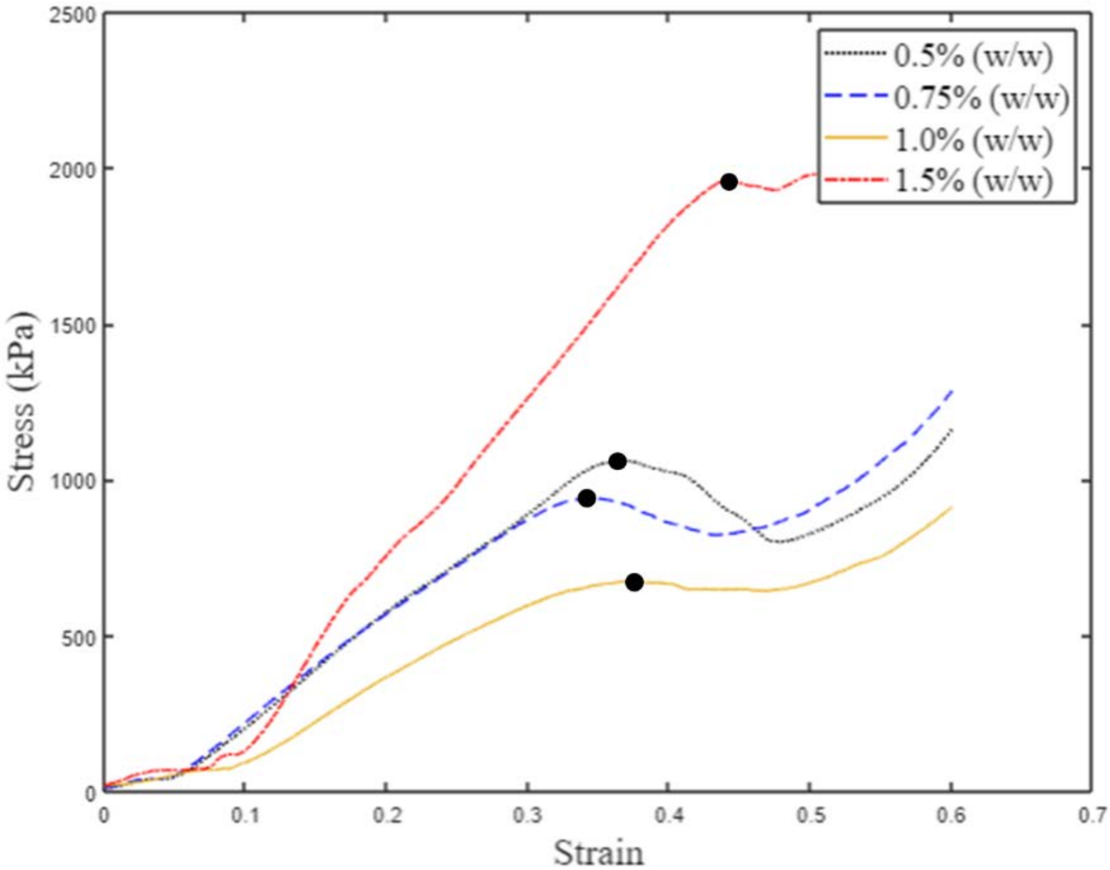

Fig. 6. Stress vs strain of bioplastic samples limited at strain 0.6 and 2250 kPa, respectively

Table 4. Ultimate strength of bioplastic samples

Bioplastic with the addition of specific amount turmeric, % (w/w)	Ultimate strength, kPa
0.50	1059.0
0.75	941.2
1.00	375.8
1.50	1957.0

The amount of turmeric affects the stiffness of the sample as the higher turmeric amount may lower the intermolecular bonding that results in a heterogeneous sample structure. It causes the stiffness of the material to decrease. This is related to fiber interaction [40] and polymerization [35]. As the result, the measured Young's modulus decreased with increasing turmeric content. These phenomena are shown in Fig. 7, in which the slope of the stress-strain curve of each sample represented Young's modulus. Based on the plot, Young's moduli of bioplastic samples of 0.50; 0.75; and 1.00% (w/w) were concluded to be 13090, 13000, and 7500 kPa, respectively (see Table 5). However, the bioplastic sample with a turmeric amount of 1.50% (w/w) showed a different trend of having two peaks. It may be correlated with the polymerization of between turmeric particles in the sample (see Fig. 4(c)), therefore the rupture characteristics affect the instability during the compression test including the stress-strain curves [41]. Hence, the stress-strain curve showed different trends of having two peaks of the slope.

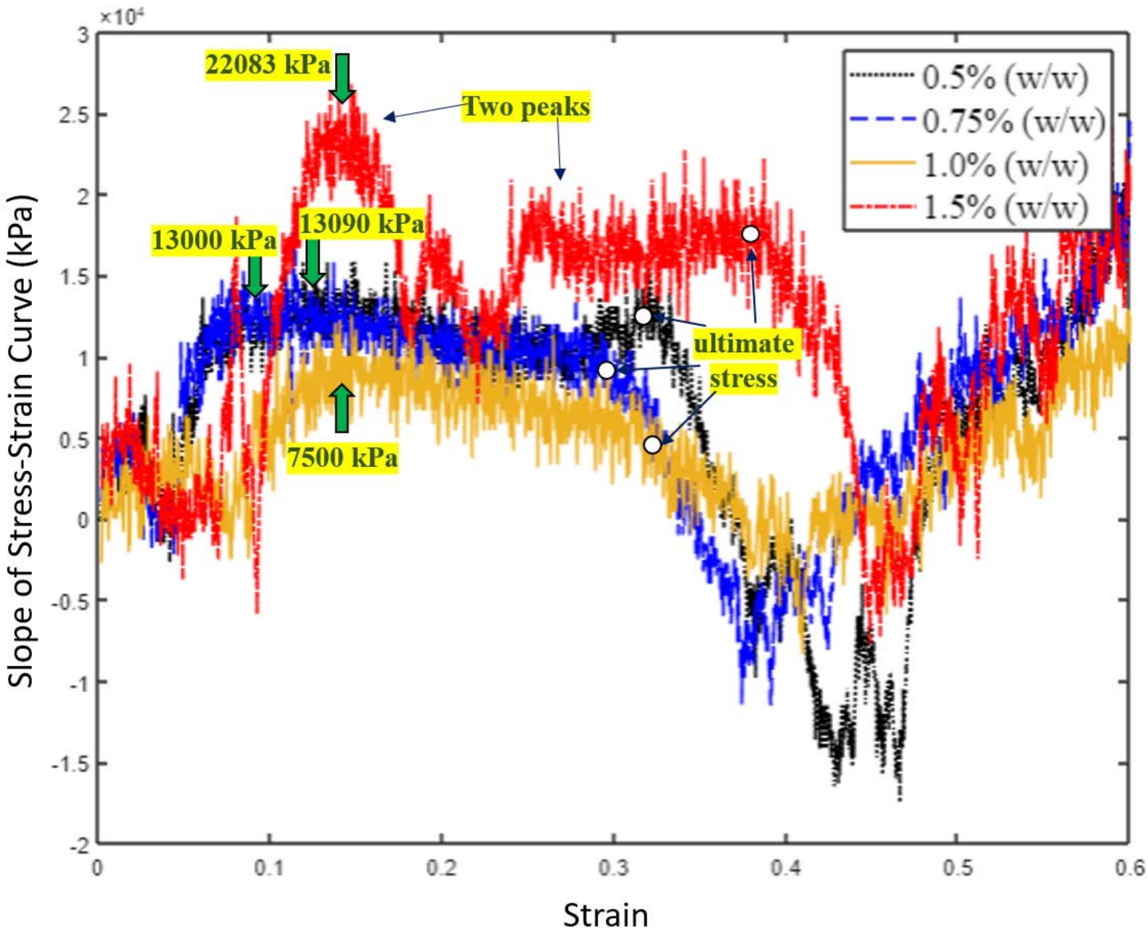

Fig. 7. Slope of stress-strain curves vs. strain of bioplastic specimens

Table 5. Ultimate strength of bioplastic samples

Bioplastic with specific amount turmeric, % (w/w)	Young's Modulus, kPa
0.50	13090
0.75	13000
1.00	7500
1.50	22083

5. Conclusion

The present work investigated biodegradability and the mechanical properties of cornstarch-based bioplastic materials by incorporating the effect of turmeric microparticles number. Based on FTIR analysis, the bioplastic soaked in water for two weeks does not demonstrate any chemical reactions, which means the dissolving process mainly causes the loss of bioplastic weight. In contrast, the bioplastic left for four weeks shows a chemical reaction caused by fungi activity. From the compressive test results, it was revealed that, for turmeric of from 0.50 to 1.00% (w/w), increasing the turmeric amount resulted in decreasing the ultimate strength value. This was likely due to the bonding between cornstarch and turmeric particles relatively weak. Furthermore, the low Young' modulus was recorded as the number of turmeric particles is high. It indicates the turmeric particles has lower rigidity than the cornstarch matrix. Due to the nature of the cracks, which always propagate to particles having lower rigidity, the bioplastic will crack more easily for higher turmeric particles. Thus, in the range of turmeric of 0.50 to 1.00% (w/w), the highest ultimate strength and highest Young's modulus of bioplastic sample were achieved by sample 0.50 (w/w) i.e. 1059 and 13090 kPa, respectively. However, different phenomena appeared for turmeric of 1.50%, in which the ultimate strength and Young’s modulus drastically increase i.e. 1957 and 22083 kPa, respectively. The turmeric particles are sufficient to create polymerization which causes the rigidity of turmeric particles to increase significantly. Thus, the crack propagates slowly in the bioplastic. The determination of turmeric amount in creating the cornstarch-based bioplastic is essential to assure the mechanical properties and biodegradability are as designed.

Acknowledgements. *This study acknowledged RISTEK BRIN for Grant-in-aid Penelitian Terapan Unggulan Perguruan Tinggi (PTUPT) and Faculty of Engineering and Technology, Sampoerna University for the mechanical testing facilities.*

References

[1] Wang Q, Cai J, Zhang L, Xu M, Cheng H, Han CC, Kuga S, Xiao J, Xiao R. A bioplastic with high strength constructed from a cellulose hydrogel by changing the aggregated structure. *Journal of Materials Chemistry A*. 2013;1(22): 6678-6686.

[2] Ezeoha SL, Ezenwanne JN. Production of biodegradable plastic packaging film from cassava starch. *IOSR Journal of Engineering*. 2013;3(10): 14-20.

[3] Emadian SM, Onay TT, Demirel B. Biodegradation of bioplastics in natural environments. *Waste management*. 2017;59: 526-536.

[4] Albuquerque PBS, Malafaia CB. Perspectives on the production, structural characteristics and potential applications of bioplastics derived from polyhydroxyalkanoates. *International Journal of Biological Macromolecules*. 2018;107: 615-625.

[5] Ramakrishnan N, Sharma S, Gupta A, Alashwal BY. Keratin based bioplastic film from chicken feathers and its characterization. *International Journal of Biological Macromolecules*. 2018;111: 352-358.

[6] Wahyuningtiyas NE, Suryanto H. Analysis of biodegradation of bioplastics made of cassava starch. *Journal of Mechanical Engineering Science and Technology (JMEST)*. 2017;1(1): 24-31.
[7] Saberi B, Chockchaisawasdee S, Golding JB, Scarlett CJ, Stathopoulos CE. Characterization of pea starch-guar gum biocomposite edible films enriched by natural antimicrobial agents for active food packaging. *Food and Bioproducts Processing*. 2017;105: 51-63.
[8] Anjum S, Gupta A, Sharma D, Gautam D, Bhan S, Sharma A, Kapil A, Gupta B. Development of novel wound care systems based on nanosilver nanohydrogels of polymethacrylic acid with Aloe vera and curcumin. *Materials Science and Engineering: C*. 2016;64: 157-166.
[9] Salahin N, Begum RA, Hossian S, Ullah MM, Alam MK. Degradation of soil properties under ginger, turmeric, aroid, and jhum rice cultivation in hilly areas of Bangladesh. *Bangladesh Journal of Agricultural Research*. 2013;38(2): 363-371.
[10] Nandiyanto ABD, Wiryani AS, Rusli A, Purnamasari A, Abdullah AG, Widiaty I, Hurriyati R. Extraction of curcumin pigment from Indonesian local turmeric with its infrared spectra and thermal decomposition properties. *IOP Conference Series: Materials Science and Engineering*. 2017;180(1): 012136.
[11] Nandiyanto ABD, Sofiani D, Permatasari N, Sucahya TN, Wiryani AS, Purnamasari A, Rusli A, Prima EC. Photodecomposition profile of organic material during the partial solar eclipse of 9 march 2016 and its correlation with organic material concentration and photocatalyst amount. *Indonesian Journal of Science and Technology*. 2016;1(2): 132-155.
[12] Meite N, Konan LK, Bamba D, Goure-Doubi BIH, Oyetola S. Structural and thermomechanical study of plastic films made from cassava-starch reinforced with kaolin and metakaolin. *Materials Sciences and Applications*. 2018;9(01): 41.
[13] Susilawati S, Rostini I, Pratama RI, Rochima E. Characterization of bioplastic packaging from tapioca flour modified with the addition of chitosan and fish bone gelatin. *World Scientific News*. 2019;135: 85-98.
[14] Nugroho FG, Nizardo NM, Saepudin E. Synthesis of citric acid crosslinked PVA/tapioca starch bioplastic reinforced with grafted cellulose. *AIP Conference Proceedings*. 2020;2242(1): 040040.
[15] Syafri E, Kasim A, Abral H, Asben A. Effect of precipitated calcium carbonate on physical, mechanical and thermal properties of cassava starch bioplastic composites. *International Journal on Advanced Science, Engineering and Information Technology*. 2017;7(5): 1950-56.
[16] Edhirej A, Sapuan SM, Jawaid M, Zahari NI. Tensile, barrier, dynamic mechanical, and biodegradation properties of cassava/sugar palm fiber reinforced cassava starch hybrid composites. *BioResources*. 2017;12(4): 7145-7160.
[17] Amri A, Ekawati L, Herman S, Yenti S, Aziz Y, Utami S. Properties enhancement of cassava starch based bioplastics with addition of graphene oxide. *IOP Conference Series: Materials Science and Engineering*. 2018;345: 012025.
[18] Zuhri LA, Muzakki MM, Rahmawati AK, Marthasari AA. Utilization of Lime Juice to Enhance Mechanical Performance of Sago-Starch Based Biofilm Reinforced Chicken Feather Keratin. *Advanced Science Letters*. 2017;23(6): 5739-5741.
[19] Syafri E, Wahono S, Irwan A, Asrofi M, Sari NH, Fudholi A. Characterization and properties of cellulose microfibers from water hyacinth filled sago starch biocomposites. *International Journal of Biological Macromolecules*. 2019;137: 119-125.
[20] Thammahiwes S, Riyajan S-A, Kaewtatip K. Preparation and properties of wheat gluten based bioplastics with fish scale. *Journal of Cereal Science*. 2017;75: 186-191.

[21] Jethoo AS. Effect of fiber reinforcement on tensile strength and flexibility of corn starch-based bioplastic. *IOP Conference Series: Materials Science and Engineering*. 2019;652(1): 012035.

[22] Agustin MB, Ahmmad B, Alonzo SMM, Patriana FM. Bioplastic based on starch and cellulose nanocrystals from rice straw. *Journal of Reinforced Plastics and Composites*. 2014;33(24): 2205-2213.

[23] Amin MR, Chowdhury MA, Kowser MA. Characterization and performance analysis of composite bioplastics synthesized using titanium dioxide nanoparticles with corn starch. *Heliyon*. 2019;5(8): e02009.

[24] Jiang B, Li S, Wu Y, Song J, Chen S, Li X, Sun H. Preparation and characterization of natural corn starch-based composite films reinforced by eggshell powder. *CyTA-Journal of Food*. 2018;16(1): 1045-1054.

[25] Ohkita T, Lee SH. Thermal degradation and biodegradability of poly (lactic acid)/corn starch biocomposites. *Journal of Applied Polymer Science*. 2006;100(4): 3009-3017.

[26] Sapei L, Padmawijaya KS, Sijayanti O, Wardhana P. Study of the influence of ZnO addition on the properties of chitosan-banana starch bioplastics. *IOP Conference Series: Materials Science and Engineering*. 2017;223(1): 012044.

[27] Maulida SM, Tarigan P. Production of starch based bioplastic from cassava peel reinforced with microcrystalline celllulose avicel PH101 using sorbitol as plasticizer. *Journal of Physics Conference Series*. 2016;710: 12012.

[28] Kasmuri N, Zait MSA. Enhancement of bio–plastic using eggshells and chitosan on potato starch based. *International Journal of Engineering and Technology*. 2018;7(3): 110-115.

[29] Silviana S, Rahayu P. Central Composite Design for Optimization of Starch-Based Bioplastic with Bamboo Microfibrillated Cellulose as Reinforcement Assisted by Potassium Chloride. *Journal of Physics: Conference Series*. 2019;1295(1): 012073.

[30] Sudharsan K, Mohan CC, Babu PAS, Archana G, Sabina K, Sivarajan M, Sukumar M. Production and characterization of cellulose reinforced starch (CRT) films. *International Journal of Biological Macromolecules*. 2016;83: 385-395.

[31] Lubis M, Gana A, Maysarah S, Ginting MHS, Harahap MB. Production of bioplastic from jackfruit seed starch (Artocarpus heterophyllus) reinforced with microcrystalline cellulose from cocoa pod husk (Theobroma cacao L.) using glycerol as plasticizer. *IOP Conference Series: Materials Science and Engineering*. 2018;309: 012100.

[32] Lubis M, Harahap MB, Ginting MHS, Sartika M, Azmi H. Production of bioplastic from avocado seed starch reinforced with microcrystalline cellulose from sugar palm fibers. *Journal of Engineering Science and Technology*. 2018;13(2): 381-393.

[33] Arini D, Ulum MS, Kasman K. Pembuatan dan pengujian sifat mekanik plastik biodegradable berbasis tepung biji durian. *Natural Science: Journal of Science and Technology*. 2017;6(3): 276-283.

[34] Triawan F, Kishimoto K, Adachi T, Inaba K, Nakamura T, Hashimura T. The elastic behavior of aluminum alloy foam under uniaxial loading and bending conditions. *Acta Materialia*. 2012;60(6-7): 3084-3093.

[35] Nandiyanto ABD, Fiandini M, Ragadhita R, Sukmafitri A, Salam H, Triawan F. Mechanical and biodegradation properties of cornstarch-based bioplastic material. *Materials Physics and Mechanics*. 2020;44(3): 380-391.

[36] Nandiyanto ABD, Oktiani R, Ragadhita R. How to read and interpret FTIR spectroscope of organic material. *Indonesian Journal of Science and Technology*. 2019;4(1): 97-118.

[37] Musso YS, Salgado PR, Mauri AN. Smart edible films based on gelatin and curcumin. *Food Hydrocolloids*. 2017;66: 8-15.

[38] Budiman BA, Adziman F, Sambegoro PL, Nurprasetio IP, Ilhamsyah R, Aziz M. The role of interfacial rigidity to crack propagation path in fiber reinforced polymer composite. *Fibers and Polymers*. 2018;19(9): 1980-1988.

[39] Budiman BA, Triawan F, Adziman F, Nurprasetio IP. Modeling of stress transfer behavior in fiber-matrix composite under axial and transverse loadings. *Composite interfaces*. 2017;24(7): 677-690.

[40] Sukrawan Y, Hamdani A, Mardani SA. Effect of bamboo weight faction on mechanical properties in non-asbestos composite of motorcycle brake pad. *Materials Physics and Mechanics*. 2019;42(3): 367-372.

[41] Nandiyanto ABD, Triawan F, Firly R, Abdullah AG, Aono Y, Inaba K, Kishimoto K. Identification of micro-mechanical characteristics of monoclinic tungsten trioxide microparticles by nanoindentation technique. *Materials Physics and Mechanics*. 2019;42(3): 323-329.